Clays and Clay Minerals, Vol. 56, No. 6, 655–659, 2008.

THE SYNTHESIS OF A PLATY CHABAZITE ANALOG FROM DELAMINATED METAKAOLIN WITH THE ABILITY TO SURFACE TEMPLATE NANOSILVER PARTICULATES

STEVEN M. KUZNICKI*, CHRISTOPHER C. H. LIN, LAN WU, HAIYAN YIN, MOHSEN DANAIE, AND DAVID MITLIN

Department of Chemical and Materials Engineering, University of Alberta, Edmonton, Alberta, Canada T6G 2V4

Abstract—Mineral chabazite has shown the unusual ability to surface template nanometal particles, especially Ag. A chabazite analog was synthesized from delaminated metakaolin. The chabazite formed retained the platy morphology of the base clay. This morphology is ideal for displaying surface-supported nanometal particles. The synthetic chabazite analog demonstrated the ability to form and support large concentrations of Ag nanoparticles, as observed in the related natural mineral. Due to greater Al content, the synthetic chabazite manifests significantly improved capacity for the formation of such Ag nanoparticles. As in the case of the mineral chabazite, surface Ag nanoparticles of high uniformity were observed in the range of 5−6 nm.

Key Words—Chabazite, Metakaolin, Nano, Silver, Zeolite.

INTRODUCTION

Nanometals are leading the nanomaterials revolution. Nanosilver is particularly interesting because of its electronic (Kim *et al*., 2007; Kolbe *et al*., 2007) and antimicrobial properties (Hilfenhaus *et al.*, 2007). Strong growth in the nanosilver market is expected as cost-effective means to generate uniform nanosilver particles are discovered (Bedrij, 2005). Mineral chabazite from Bowie, Arizona, (Eyde *et al.*, 1987) has recently been reported to have the unusual property of generating large concentrations (up to 20+ wt.%) of uniform Ag nanoparticles on its surface which auto-form when Ag-exchanged chabazite is thermally reduced (Kuznicki *et al.*, 2007a). These Ag nanoparticles (as small as 2.5 nm) are showing promise in applications ranging from anti-fungal medicine to removal of mercury from flue gases (Kuznicki *et al.*, 2007a). A recent report indicated that similar Ag nanoparticles undergo a size-dependent interaction with HIV-1 which may inhibit the virus from binding to host cells (Elechiguerra *et al.*, 2005). Besides being an antimicrobial agent, nanoparticles of Ag also exhibit a unique ability for the adsorption of 'inert' gases such as Xe (Kuznicki *et al.*, 2007b) and Ar (Anson *et al.*, 2008). The unusual propensity to form and support metallic (Ag) nanoparticles on chabazite is attributed to the mineral's strong surface polarization and platy morphology (Kuznicki *et al.*, 2007c).

Mineral chabazite is a highly polarizing molecular sieve adsorbent found in many deposits throughout the world, including a large, commercially exploited deposit in Bowie, Arizona (Eyde *et al.*, 1987). The chabazite ore found at Bowie is ~70% chabazite combined with 15% clinoptilolite, some erionite, and a mixture of amorphous aluminosilicate species. Mineral chabazite typically has a Si/Al ratio of 3, while synthetic chabazites can be prepared with Si/Al ratios approaching 1.0 (Kuznicki and Whyte, 1988), significantly increasing the cation exchange capacity (CEC) of the material. A process has been developed by which the raw ore can be upgraded to essentially pure, high-Al synthetic chabazite; the clinoptilolite and much of the other siliceous contaminant material are dissolved and recrystallized into chabazite (Kuznicki *et al*., 2007c). During the preparation process, the structure of the material is completely rearranged on a molecular level to form a three-dimensional porous chabazite molecular sieve, while the gross macrostructure of the clay platelet is retained, yielding an ideal surface on which to display nanometal particles. Using this technique, a purer, greater-capacity synthetic chabazite analog could potentially be prepared from clay-based starting materials with a platy morphology, in the hope of retaining this morphology in the crystalline zeolite support. Metakaolin, a widely employed reactant in the synthesis of *in situ* zeolite aggregates (Liu and Pinnavaia, 2004), would appear to be a prime candidate if used in a delaminated form.

The synthesis of a high-purity chabazite analog from delaminated metakaolin, which retains the base material's platy morphology, is reported here. Such morphology would be ideal for displaying Ag nanoparticles for many applications. With increasing Al content (*vs*. the natural mineral), greater Ag loadings might also be expected. If such materials readily templated nanosilver particles, as seen in the mineral analog, a new generation of nanosilver materials (prepared much more economically than by current nanosilver synthesis techniques, including vapor deposition (Nepikjo *et al*.,

* E-mail address of corresponding author:
steve.kuznicki@ualberta.ca
DOI: 10.1346/CCMN.2008.0560606

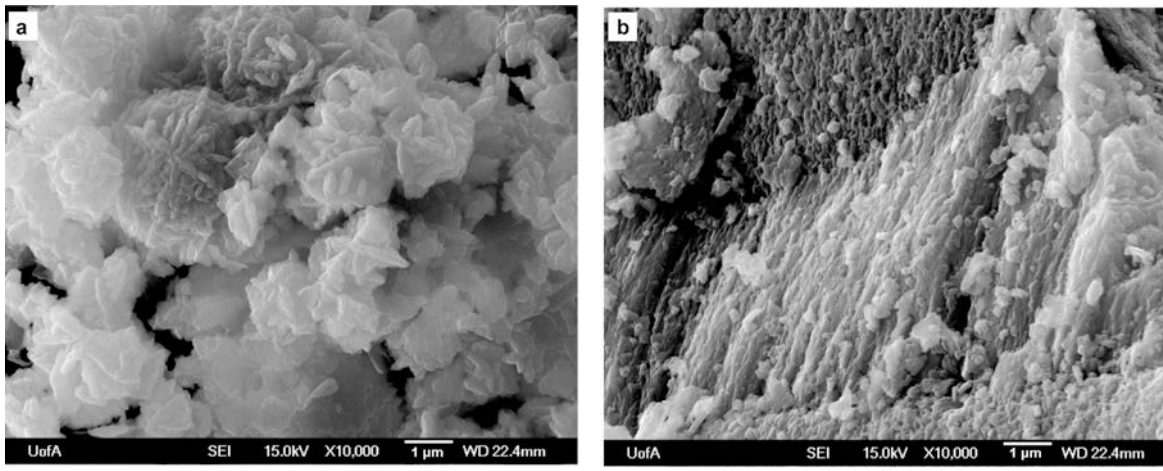

Figure 1. Surface SEM images of the: (a) synthetic chabazite analog; and (b) mineral chabazite.

2000) and atomic sputtering (Chandra *et al.*, 1999)) might result in new opportunities for the nanomaterials revolution.

MATERIALS AND METHODS

Materials

Sedimentary Na chabazite from the Bowie deposit, Arizona, (Eyde *et al.*, 1987) was obtained from GSA Resources of Tucson, Arizona. The synthetic chabazite analog was synthesized using delaminated metakaolin, obtained from Engelhard Corporation, as the primary reactant. A typical mixture of the synthetic chabazite analog involved mixing 90 g of metakaolin, 100 g of Na silicate (28.8% SiO_2, 9.14% Na_2O, Fisher), 24 g of Na hydroxide (97+% NaOH, Fisher), and 340 g of de-ionized water, with 30 g of finely powdered (<75 µm) mineral Na chabazite added as a seeding agent. This reaction mixture had a net molar composition of 3.48 SiO_2:1 Al_2O_3:0.93 Na_2O:47.61 H_2O. The mixture was stirred in an orbital mixer for 1 h and aged at 50ºC for 24 h. The mixture was then crystallized statically for 72 h at 100ºC. The resultant material was washed thoroughly with de-ionized water and dried in a forced-air oven at 80ºC.

Ag ion-exchange for both natural chabazite and the synthetic chabazite analog was accomplished by exposing the materials to an excess of aqueous Ag nitrate statically at 80ºC for 16 h. The Ag is initially exchanged as ions. Silver exchanges very well into high-Al chabazites and is essentially quantitatively exchanged (Sun and Seff, 1994). The resultant materials were washed with de-ionized water, dried at 80ºC, and annealed at 150ºC for 4 h to convert the Ag ions into surface-supported Ag nanoparticles.

Characterization

Powder X-ray diffraction analysis (XRD) was used for phase identification. The XRD data were collected using a Rigaku Geigerflex 2173 with a vertical goniometer equipped with a diffracted-beam graphite monochromator for filtration of reflections due to K-β wavelengths. Peak identification was performed using standard literature data (Breck, 1974).

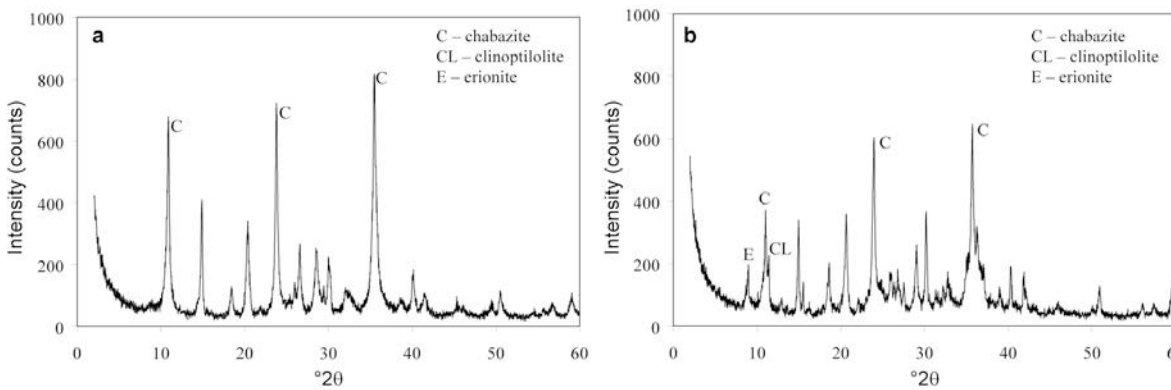

Figure 2. Powder XRD patterns of the: (a) synthetic chabazite analog; and (b) mineral chabazite.

https://doi.org/10.1346/CCMN.2008.0560606 Published online by Cambridge University Press

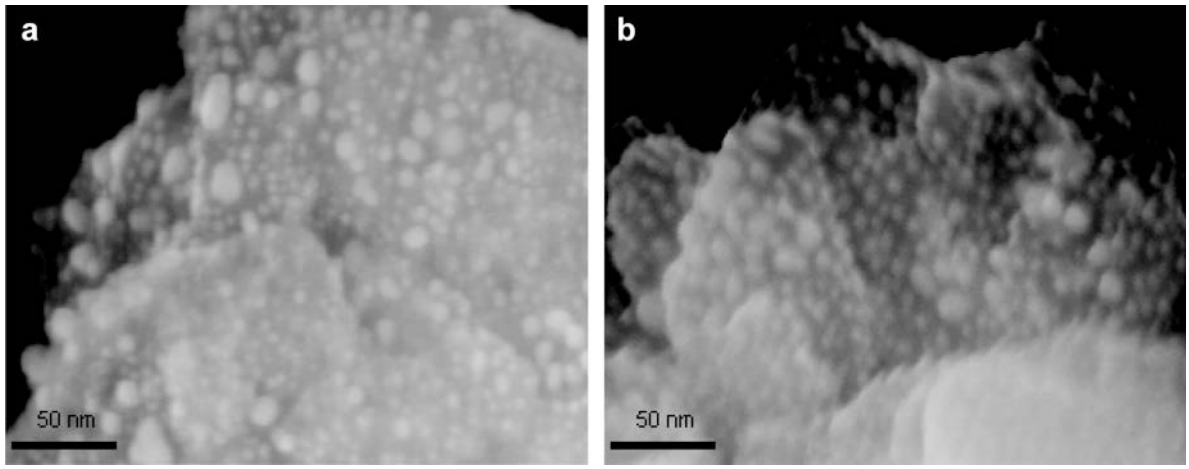

Figure 3. SEM images of Ag nanoparticles on the: (a) synthetic chabazite analog; and (b) mineral chabazite.

The external surface area was measured using a multi-point BET technique, employing N_2 as the adsorbate in a Quantachrome Autosorb-1 unit.

Scanning electron microscopy (SEM) supplemented with energy dispersive X-ray spectroscopy (EDX) was used for the characterization of the Ag nanoparticles. The data were collected using a Field Emission Hitachi S4800 at 15 kV accelerating voltage with secondary electrons as signals. Transmission electron microscopy (TEM) was performed on a Hitachi H-7000 unit. Bulk elemental analyses of the samples were determined using EDX. Particle size analysis was performed using the program *ImageJ*, a public domain Java image processing program developed (Rasband, 2008) at the National Institute of Mental Health, Research Services Branch (USA).

RESULTS AND DISCUSSION

Scanning electron microscopy analysis of the synthetic chabazite analog (Figure 1a) indicated that polycrystalline particles formed as submicrometer crystallites with a layered morphology. The external surface area of the synthetic chabazite analog (18.43 m^2/g) was nearly identical to the starting delaminated metakaolin (17.14 m^2/g). The clay-derived chabazite analog exhibited a distinct surface morphology reminiscent of the original clay. Energy dispersive X-ray analysis indicated that the synthetic chabazite analog was enriched with structural Al exhibiting a Si/Al ratio of 1.46, as compared to the raw mineral at 3.30.

Powder XRD patterns of the synthetic chabazite (Figure 2a) indicated that the material was very pure and crystalline. In contrast to the Bowie mineral chabazite (Figure 2b), where a significant amount of crystalline contaminants such as clinoptilolite and erionite were present, the clay-derived chabazite was essentially free of contaminants, which presumably re-crystallized to the chabazite analog during the crystallization process. From XRD, the synthetic chabazite analog appeared much more homogenous than the natural mineral from which it was derived.

Typically, kaolin has a very low CEC but digestion in an alkaline silicate solution transformed kaolinite into a relatively high-Al chabazite. While the synthetic chabazite analog maintained the platy morphology of the original kaolin, the CEC of the analog increased. Based on elemental analysis of the metakaolin-derived synthetic chabazite, the theoretical CEC value for the new material was 6.11 meq/g, significantly better than that of mineral chabazite (3.68 meq/g). The experimental CEC values, derived from ion-exchange measurements, were similar: 5.40 meq/g for synthetic chabazite and 3.74 meq/g for mineral chabazite.

From the SEM images of heat-treated, Ag-exchanged samples (Figure 3), Ag nanoparticles appeared to cover the surfaces of both the synthetic analog and mineral chabazite. Elemental analysis utilizing EDX indicated

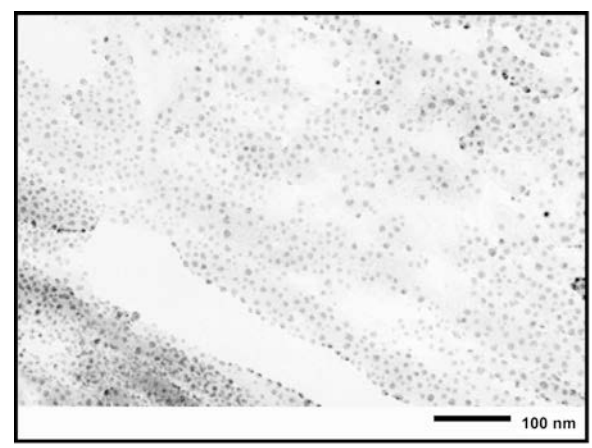

Figure 4. TEM image of Ag nanoparticles on the synthetic chabazite analog.

https://doi.org/10.1346/CCMN.2008.0560606 Published online by Cambridge University Press

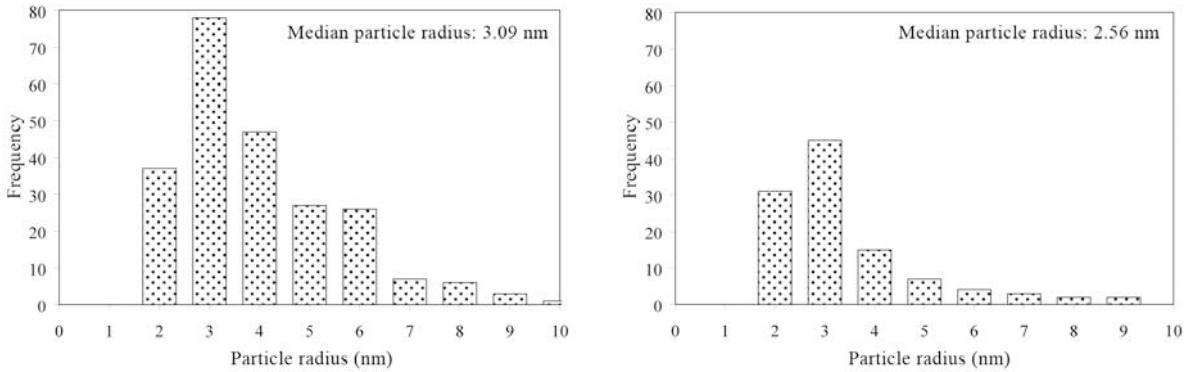

Figure 5. Particle-size distribution of Ag nanoparticles on the: (a) synthetic chabazite analog; and (b) mineral chabazite.

that the synthetic chabazite analog contained 39 wt.% Ag, compared to 27 wt.% Ag in the mineral chabazite, which conformed to the results of subsequent bulk analysis. This was consistent with the increased cation-exchange capacity associated with increased structural Al in the synthetic chabazite analog. The well attached particles, formed on the surface of the synthetic chabazite analog, appeared even more uniform when viewed using TEM (Figure 4), where a narrow size distribution of ~5–6 nm was observed.

The electron diffraction data indicate that the Ag nanoparticles were crystalline, metallic Ag (Lin *et al.*, in press), while ^{109}Ag NMR indicates that no Ag^+ remained associated with the chabazite after annealing (Liu *et al.*, in press).

The mechanism for the formation of these crystalline, metallic Ag nanoparticles has been the subject of a significant research effort (Sun and Seff, 1994; Kuznicki *et al.*, 2007a; Liu *et al.*, 2008; and references therein). When Ag-exchanged zeolite is heated, Ag molecular aggregates are formed. Aggregate formation is followed by the migration of the reduced metal from the interior cavities to the surface of zeolite crystals. This phenomenon generally continues until micrometer-sized pools of metal are observed (Sun and Seff, 1994). The highly-charged surfaces of chabazite-like species, however, function to quantitatively fix reduced Ag as nm-sized particles (Kuznicki 2007a; Liu *et al.*, in press). It is posited that H^+ (from water) is left behind to compensate for Ag^+ charge as Ag is reduced. Water is a key ingredient in this process, as it supplies both the oxygen required to form an unstable Ag oxide (which decomposes to form the nanometal), and the charge-compensating H^+. While the nanoparticles will form as the Ag ion-exchanged chabazite dries at even lower temperatures, the process appears to be complete after drying at 150ºC.

The particle-size distributions of the Ag nanoparticles on the synthetic analog and Bowie mineral chabazite were comparable (Figure 5). Statistical analysis indicated that the median particle radius was similar for both materials, ~3.1 nm for the synthetic support and 2.6 nm for the mineral.

CONCLUSIONS

An Al-enriched synthetic chabazite analog was derived from delaminated metakaolin, retaining the starting material's external surface area and morphology. This synthetic chabazite analog was substantially purer and had a greater Al content (and corresponding CEC) than the mineral from which it was derived. The ability to surface template Ag nanoparticles previously reported on mineral chabazite was observed to occur on the purified synthetic analog with substantially greater Ag loadings. Such materials may represent a new and economical way to generate nanosilver and potentially other nanometals, increasing their areas of potential utility and impact.

ACKNOWLEDGMENTS

The authors are grateful for support and encouragement from the Canada Research Chair in Molecular Sieve Nanomaterials, the Alberta Ingenuity Fund, and GSA Resources of Tucson, Arizona. They also acknowledge Dr Marek Malac, Julie Qian, and Daniel Salamon from the Canadian National Institute for Nanotechnology (NINT) for assistance with the microscopy.

REFERENCES

Anson, A., Kuznicki, S.M., Kuznicki, T., Haastrup, T., Wang, Y., Lin, C.C.H., Sawada, J.A., Eyring, E.M., and Hunter, D. (2008) Adsorption of argon, oxygen, and nitrogen on silver exchanged ETS-10 molecular sieve. *Microporous and Mesoporous Materials*, **109**, 577–580.

Bedrij, C. (2005) *Nanotechnology Industry Review*. Griffin Securities Inc, New York.

Breck, D.W. (1974) *Zeolite Molecular Sieves: Structure, Chemistry and Use*. Wiley-Interscience Publication, New York, 771 pp.

Chandra, R., Taneja, P., John, J., Ayyub, P., Dey, G.K., and Kulshreshtha, S.K. (1999) Synthesis and TEM study of nanoparticles and nanocrystalline thin films of silver high-pressure sputtering. *Nanostructured Materials*, **11**, 1171–1179.

Elechiguerra, J.L., Burt, J.L., Morones, J.R., Camacho-Bragado, A., Gao, X., Lara, H.H., and Yacaman, M.J. (2005) Interaction of silver nanoparticles with HIV-1. *Journal of Nanobiotechnology*, **3**, 1–10.

Eyde, T.H., Sheppard, R.A., and Barclay, C.S.V. (1987) *Geology, Mineralogy, and Mining of the Bowie Zeolite*

Deposit Graham and Cochise Counties, Arizona. ZeoTrip '87, International Committee on Natural Zeolites.

Hilfenhaus, P., Heike, J., and Buettner, H. (2007) *Antimicrobial wound dressing*. US Patent 7,270,721.

Kim, N.S., Amert, A.K., Woessner, S.M., Decker, S., Kang, S.M., and Han, K.N. (2007) Effect of metal powder packing on the conductivity of nanometal ink. *Journal of Nanoscience and Nanotechnology*, **7**, 3902–3905.

Kolbe, J., Arp, A., Calderone, F., Meyer, E.M., Meyer, W., Schaefer, H., and Stuve, M. (2007) Inkjettable conductive adhesive for use in microelectronics and microsystems technology. *Microelectronics Reliability*, **47**, 331–334.

Kuznicki, S.M. and Whyte, Jr., J.R. (1988) *Ion-exchange agent and use thereof in extracting heavy metals from aqueous solutions*. US Patent 5,071,804, filed Sep 8, 1988, and issued Dec 10, 1991.

Kuznicki, S.M., Kelly, D.J.A., Bian, J., Lin, C.C.H., Chen, J., Liu, Y., Mitlin, D., and Xu, Z. (2007a) Metal nanodots formed and supported on chabazite and chabazite-like surfaces. *Microporous and Mesoporous Materials*, **103**, 309–315.

Kuznicki, S.M., Anson, A., Koenig, A., Kuznicki, T.M., and Haastrup, T. (2007b) Xenon adsorption on modified ETS-10. *Journal of Physical Chemistry C*, **111**, 1560–1562.

Kuznicki, S.M., Lin, C.C.H., Bian, J., and Anson, A. (2007c) Chemical upgrading of Bowie, Arizona sedimentary Na-chabazite. *Clays and Clay Minerals*, **55**, 235–238.

Lin, C.C.H., Danaie, M., Liu, Y., Mitlin, D., Kuznicki, S.M., and Eyring, E.M. (2009) Thermally stable silver nanoparticles formed on a zeolite surface show multiple crystal twinning (in press).

Liu, Y. and Pinnavaia, T.J. (2004) Metakaolin as a reagent for the assembly of mesoporous aluminosilicates with hexagonal, cubic and wormhole framework structures from protofaujasitic nanoclusters. *Journal of Materials Chemistry*, **14**, 3416–3420.

Liu, Y., Chen, F., Kuznicki, S.M., Wasylishen, R.E. and Xu, Z. (2009) A novel method to control the size of silver nanoparticles formed on silver chabazite. *Journal of Nanoscience and Nanotechnology*, (in press).

Nepijko, S.A., Ievlev, D.N., Schulze, W., Urban, J., and Ertl, G. (2000) Growth of rodlike silver nanoparticles by vapor deposition of small clusters. *ChemPhysChem*, **1**, 140–142.

Rasband, W. (2008) ImageJ: Image processing and analysis in Java. http://rsbweb.nih.gov/ij/.

Sun, T. and Seff, K. (1994) Silver clusters and chemistry in zeolites. *Chemical Reviews*, **94**, 857–870.

(*Received 2 November 2007; revised 26 August 2008; Ms. 0094*)